JFM RAPIDS
journals.cambridge.org/rapids

The boundary integral formulation of Stokes flows includes slender-body theory

Lyndon Koens[1] **and Eric Lauga**[1,†]

[1]Department of Applied Mathematics and Theoretical Physics, University of Cambridge, Wilberforce Road, Cambridge CB3 0WA, UK

The incompressible Stokes equations can classically be recast in a boundary integral (BI) representation, which provides a general method to solve low-Reynolds-number problems analytically and computationally. Alternatively, one can solve the Stokes equations by using an appropriate distribution of flow singularities of the right strength within the boundary, a method that is particularly useful to describe the dynamics of long slender objects for which the numerical implementation of the BI representation becomes cumbersome. While the BI approach is a mathematical consequence of the Stokes equations, the singularity method involves making judicious guesses that can only be justified *a posteriori*. In this paper, we use matched asymptotic expansions to derive an algebraically accurate slender-body theory directly from the BI representation able to handle arbitrary surface velocities and surface tractions. This expansion procedure leads to sets of uncoupled linear equations and to a single one-dimensional integral equation identical to that derived by Keller & Rubinow (*J. Fluid Mech.*, vol. 75, 1976, p. 705) and Johnson (*J. Fluid Mech.*, vol. 99, 1979, p. 411) using the singularity method. Hence, we show that it is a mathematical consequence of the BI approach that the leading-order flow around a slender body can be represented using a distribution of singularities along its centreline. Furthermore, when derived from either the single-layer or the double-layer modified BI representation, general slender solutions are only possible in certain types of flow, in accordance with the limitations of these representations.

Key words: boundary integral methods, low-Reynolds-number flows, slender-body theory

1. Introduction

The low-Reynolds-number hydrodynamics of viscous fluids is accurately captured by the incompressible Stokes equations,

$$-\nabla p + \mu \nabla^2 \boldsymbol{u} + \boldsymbol{f} = \boldsymbol{0}, \tag{1.1}$$

† Email address for correspondence: e.lauga@damtp.cam.ac.uk

$$\nabla \cdot \boldsymbol{u} = 0, \tag{1.2}$$

where $\boldsymbol{u}$ is the velocity of the fluid, p is the dynamic pressure, μ is the dynamic viscosity and $\boldsymbol{f}$ is any external force density acting on the fluid (Kim & Karrila 2005).

The Green's function for these equations, $\boldsymbol{G}(\boldsymbol{R})$, is called the stokeslet and represents the flow from a point force of strength $\boldsymbol{F}$. In an unbounded fluid, the associated flow $\boldsymbol{u}_S(\boldsymbol{x})$ at position $\boldsymbol{x}$ resulting from a force located at $\boldsymbol{x}_0$ takes the form

$$8\pi\mu\boldsymbol{u}_S(\boldsymbol{x}) = \boldsymbol{G}(\boldsymbol{R}) \cdot \boldsymbol{F} = \frac{\boldsymbol{I} + \hat{\boldsymbol{R}}\hat{\boldsymbol{R}}}{|\boldsymbol{R}|} \cdot \boldsymbol{F}, \tag{1.3}$$

where $\boldsymbol{I}$ is the identity tensor, $\boldsymbol{R} = \boldsymbol{x} - \boldsymbol{x}_0$ is a vector from the point force to $\boldsymbol{x}$, $|\boldsymbol{R}|$ is the magnitude of $\boldsymbol{R}$ and $\hat{\boldsymbol{R}}$ is a unit vector in the direction of $\boldsymbol{R}$. This stokeslet allows the velocity at any point within the fluid, $\boldsymbol{x}$, to be expressed as (Pozrikidis 1992)

$$8\pi\mu\boldsymbol{u}(\boldsymbol{x}) = \iint_S \mathrm{d}S(\boldsymbol{x}_0)[\boldsymbol{G}(\boldsymbol{R}) \cdot \boldsymbol{f}(\boldsymbol{x}_0)] + \mu \iint_S \mathrm{d}S(\boldsymbol{x}_0)[\boldsymbol{U}(\boldsymbol{x}_0) \cdot \boldsymbol{T}(\boldsymbol{R}) \cdot \hat{\boldsymbol{n}}_S(\boldsymbol{x}_0)], \tag{1.4}$$

where $\boldsymbol{U}(\boldsymbol{x}_0)$ is the surface velocity at $\boldsymbol{x}_0$, $\iint_S \mathrm{d}S(\boldsymbol{x}_0)$ are integrals over the boundaries S of the fluid, $\hat{\boldsymbol{n}}_S$ is the surface normal pointing out of the fluid, $\boldsymbol{f}(\boldsymbol{x}_0) = \boldsymbol{\sigma}(\boldsymbol{x}_0) \cdot \hat{\boldsymbol{n}}_s$ is the surface traction on the fluid at $\boldsymbol{x}_0$, $\boldsymbol{\sigma}(\boldsymbol{x}_0)$ is the fluid stress at $\boldsymbol{x}_0$ and $\boldsymbol{T}(\boldsymbol{R})$ is the stress tensor generated from the stokeslet (Pozrikidis 1992). In an unbounded fluid, the stress tensor, $\boldsymbol{T}(\boldsymbol{R})$, has the form

$$\boldsymbol{T}(\boldsymbol{R}) = -6\frac{\hat{\boldsymbol{R}}\hat{\boldsymbol{R}}\hat{\boldsymbol{R}}}{|\boldsymbol{R}|^2}. \tag{1.5}$$

In the limit that $\boldsymbol{x}$ approaches the boundary in (1.4), the integral equation becomes

$$4\pi\mu\boldsymbol{U}(\boldsymbol{x}) = \iint_S \mathrm{d}S(\boldsymbol{x}_0)[\boldsymbol{G}(\boldsymbol{R}) \cdot \boldsymbol{f}(\boldsymbol{x}_0)] + \mu \iint_S^{PV} \mathrm{d}S(\boldsymbol{x}_0)[\boldsymbol{U}(\boldsymbol{x}_0) \cdot \boldsymbol{T}(\boldsymbol{R}) \cdot \hat{\boldsymbol{n}}_S(\boldsymbol{x}_0)], \tag{1.6}$$

where $\iint^{PV} \mathrm{d}S(\boldsymbol{x}_0)$ is the Cauchy principal value of the integral. The above equation provides a relationship between the surface traction, $\boldsymbol{f}(\boldsymbol{x}_0)$, and the surface velocity, $\boldsymbol{U}(\boldsymbol{x}_0)$, and thus, together with (1.4), completely determines the flow. Equations (1.4) with (1.6) are called the boundary integral (BI) representation of Stokes flow. It should be noted that the first integral on the right-hand side of (1.4) is usually called the single-layer potential while the second integral is referred to as the double-layer potential.

Alternatively, Stokes flow problems can be solved through the singularity representation method, where fundamental flow singularities are placed outside the fluid region to exactly satisfy all boundary conditions. For an isolated body in flow, this means that these singularities are placed inside the body. One difficulty of this method is that, in general, the details of the singularities needed to satisfy the boundary conditions (type, location and strength) are not known *a priori*. As a result, exact solutions using this method are only known for simple shapes. For example, Chwang & Wu (1975) showed that the rigid body motion of a prolate ellipsoid of arbitrary aspect ratio can be represented by a line distribution of four singularities placed between the foci of the body. In general, however, infinite singularities may be needed to represent the desired flow (Kim & Karrila 2005).

In the limit of very large aspect ratios, a prolate ellipsoid becomes a long slender body with a straight centreline. For such slender shapes, numerical implementations of the BIs tend to require a high resolution to resolve both length scales of the body, and so many singularity representation methods, called slender-body theories (SBTs), have been developed to overcome this difficulty (Batchelor 1970; Cox 1970; Clarke 1972; Keller & Rubinow 1976; Lighthill 1976; Johnson 1979; Sellier 1999; Götz 2000; Koens & Lauga 2016, 2017). Early SBTs used a line of stokeslets to represent the rigid body motion of the object, and typically expanded the system in orders of $1/\ln(r_f/\ell)$, where 2ℓ is the total length of the slender body and r_f is its maximum radius (Batchelor 1970; Cox 1970). Clarke (1972) showed that, for straight slender bodies, the equations of Batchelor (1970) could also be derived by expanding the single-layer BI in powers of $1/\ln(r_f/\ell)$.

Algebraically accurate SBTs were later developed by including higher-order singularities, often inspired by the exact solution for a prolate ellipsoid (Keller & Rubinow 1976; Lighthill 1976; Johnson 1979). Algebraic SBTs typically represent the flow around a rigid body through a one-dimensional Fredholm equation of the second kind. For example, the SBT of Keller & Rubinow (1976) can be written as

$$8\pi \boldsymbol{U}(s) = \int_{-\ell}^{\ell} \left(\frac{\boldsymbol{I} + \hat{\boldsymbol{R}}_0 \hat{\boldsymbol{R}}_0}{|\boldsymbol{R}_0|} \cdot \boldsymbol{f}(s') - \frac{\boldsymbol{I} + \hat{\hat{\boldsymbol{t}}}\hat{\boldsymbol{t}}}{|s' - s|} \cdot \boldsymbol{f}(s) \right) \mathrm{d}s'$$
$$+ [L_{SBT}(\boldsymbol{I} + \hat{\hat{\boldsymbol{t}}}\hat{\boldsymbol{t}}) + \boldsymbol{I} - 3\hat{\hat{\boldsymbol{t}}}\hat{\boldsymbol{t}}] \cdot \boldsymbol{f}(s), \tag{1.7}$$

where $s \in [-\ell, \ell]$ is the arclength of the centreline, $\boldsymbol{r}(s)$ is the centreline of the slender body, $\boldsymbol{R}_0 = \boldsymbol{r}(s) - \boldsymbol{r}(s')$, $\hat{\boldsymbol{t}}$ is the unit vector tangent to the centreline, $\boldsymbol{f}(s)$ is the hydrodynamic force density on the filament, $\boldsymbol{U}(s)$ is the velocity of the body centreline, $L_{SBT} = \ln[4\ell^2(1 - s^2)/(r_f^2 \rho^2)]$ and $r_f \rho(s)$ is the radius of the filament at s (figure 1). Note that in order for equation (12) of Keller & Rubinow (1976) to be written in the form of (1.7) one needs to collect all velocity terms on the left, all force terms on the right, and recognise that $\boldsymbol{i} = \hat{\boldsymbol{t}}$, $\boldsymbol{\alpha} = \boldsymbol{f}$, and $\boldsymbol{j}$ is a projection operator taking the components perpendicular to $\hat{\boldsymbol{t}}$ (i.e. $\boldsymbol{jj} = \boldsymbol{I} - \hat{\boldsymbol{t}}\hat{\boldsymbol{t}}$). Later, Johnson (1979) derived the same integral equations by placing a distribution of stokeslets and potential source dipoles (defined as half the Laplacian of a stokeslet) along the centreline of the body and expanding the resultant flow in the slender limit. In doing so, he also created a set of equations that were accurate to order $(r_f/\ell)^2$ and showed that $\boldsymbol{f}(s)$ determined the force per unit length to order $r_f^2 \log(r_f/\ell)/\ell^2$. Slender-body theories have proved crucial in understanding the hydrodynamics and rheology of filaments (Tornberg & Shelley 2004; Tornberg & Gustavsson 2006), the swimming of microorganisms (Barta & Liron 1988; Myerscough & Swan 1989; Smith *et al.* 2009; Koens & Lauga 2014) and the behaviour of active systems (Guo *et al.* 2018).

In this paper, we demonstrate that a general SBT can be derived directly from the BI representation for Stokes flows by algebraically expanding the kernels of the BI representation in a matched asymptotic expansion. The equation we obtain relating the mean force per unit length to the centreline velocity is identical to the Keller–Rubinow–Johnson SBT equation (KRJ-SBT), equation (1.7), thereby revealing that the BI representation reduces to the singularity representation for slender bodies in the appropriate limits. These SBT equations are a direct consequence of the Stokes equations, can handle arbitrary surface velocities and forces, and require no assumptions about singularity types, locations or strengths. The modified single-layer and double-layer BI equations are also addressed, showing that corresponding SBT solutions only exist when specific conditions are met.
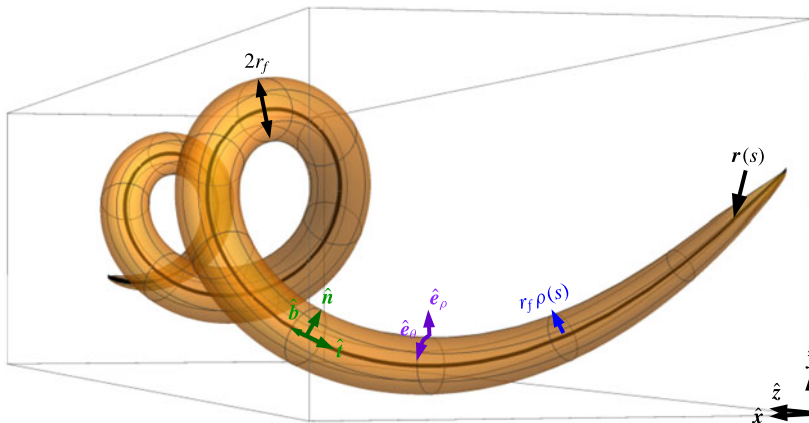
FIGURE 1. Geometric representation of a slender body of length 2ℓ and maximum radius r_f. Here, $\boldsymbol{r}(s)$ is the position of the centreline, $r_f\rho(s) \in [0, r_f]$ is the radius of the body, $\hat{\boldsymbol{t}}$ is the tangent to the centreline, $\hat{\boldsymbol{n}}$ is the normal to the centreline, $\hat{\boldsymbol{b}}$ is the binormal to the centreline, $\hat{\boldsymbol{e}}_\rho(s, \theta) = \cos[\theta - \theta_i(s)]\hat{\boldsymbol{n}}(s) + \sin[\theta - \theta_i(s)]\hat{\boldsymbol{b}}(s)$ is the radial unit vector and $\hat{\boldsymbol{e}}_\theta(s, \theta) = -\sin[\theta - \theta_i(s)]\hat{\boldsymbol{n}}(s) + \cos[\theta - \theta_i(s)]\hat{\boldsymbol{b}}(s)$ is the polar unit vector.

2. Geometry of slender body

Points on the surface of a filamentous body of total arclength 2ℓ and a circular cross-section of maximum radius r_f can be described using the arclength $s \in [-\ell, \ell]$ as

$$\boldsymbol{S}(s, \theta) = \boldsymbol{r}(s) + r_f\rho(s)\hat{\boldsymbol{e}}_\rho(s, \theta), \qquad (2.1)$$

where $\boldsymbol{r}(s)$ is the centreline of the filament, $r_f\rho(s) \in [0, r_f]$ is the cross-sectional radius of the body at s, $\hat{\boldsymbol{e}}_\rho(s, \theta) = \cos[\theta - \theta_i(s)]\hat{\boldsymbol{n}}(s) + \sin[\theta - \theta_i(s)]\hat{\boldsymbol{b}}(s)$ is the local radial vector perpendicular to the centreline tangent $\hat{\boldsymbol{t}}(s)$, $\hat{\boldsymbol{n}}(s)$ denotes the normal to the centreline and $\hat{\boldsymbol{b}}(s)$ is the binormal, $\theta \in [-\pi, \pi]$ is the azimuthal angle of the cross-section and $\theta_i(s)$ accounts for the torsion of the curve (figure 1). We choose $\theta_i(s)$ to satisfy

$$\frac{\mathrm{d}\theta_i}{\mathrm{d}s} = \tau(s), \qquad (2.2)$$

such that

$$\frac{\mathrm{d}\hat{\boldsymbol{e}}_\rho}{\mathrm{d}s} = -\kappa(s)\cos[\theta - \theta_i(s)]\hat{\boldsymbol{t}}, \qquad (2.3)$$

where $\kappa(s)$ and $\tau(s)$ are the curvature and torsion of the centreline respectively. This parametrisation describes a filament if $r_f < \ell$ and a slender body in the limit $r_f \ll \ell$.

3. Asymptotic expansion of the BIs

In this section, we expand the BI representation, equation (1.6), for small values of $\epsilon \equiv r_f/\ell$ to derive a set of slender-body equations. This is done by performing a matched asymptotic expansion on the integral kernels before evaluating the integrals. A similar derivation was used by Johnson (1979) and Götz (2000) to derive their respective SBTs but was applied to a prescribed line of singularities rather than to the

full BI equations. As the BI is divided into single-layer and double-layer components, the kernels to expand are

$$K_t \equiv \left| \frac{\mathrm{d}S}{\mathrm{d}s'} \times \frac{\mathrm{d}S}{\mathrm{d}\theta'} \right| G(R) \cdot f(x_0) = \rho(s') \frac{I + \hat{R}\hat{R}}{|R|} \cdot f(s', \theta'), \tag{3.1}$$

$$K_s \equiv \left| \frac{\mathrm{d}S}{\mathrm{d}s'} \times \frac{\mathrm{d}S}{\mathrm{d}\theta'} \right| [U(x_0) \cdot T(R) \cdot \hat{n}_s(x_0)] = -6\epsilon \rho(s') U(s', \theta') \cdot \frac{\hat{R}\hat{R}\hat{R}}{|R|^2} \cdot \hat{n}_S(s', \theta'), \tag{3.2}$$

where K_t is the single-layer kernel, K_s is the double-layer kernel, $U(s, \theta)$ is the surface velocity of the body at (s, θ) and

$$R \equiv S(s, \theta) - S(s', \theta') = R_0(s, s') + \epsilon[\rho(s)\hat{e}_\rho(s, \theta) - \rho(s')\hat{e}_\rho(s', \theta')]. \tag{3.3}$$

In the above, we have scaled all lengths by half of the arclength of the body, ℓ, velocities by a typical velocity, U, and the surface traction by a characteristic force per unit surface area, $\mu \ell U/(r_f \ell)$. Furthermore, the slender surface integration factor,

$$\left| \frac{\partial S(s', \theta')}{\partial s'} \times \frac{\partial S(s', \theta')}{\partial \theta'} \right| = \epsilon \rho(s') + O(\epsilon^2), \tag{3.4}$$

has also been included in the kernels in order to reduce the surface integration to a double integral over $s' \in [-1, 1]$ and $\theta' \in [-\pi, \pi]$. The integration factor is obtained by recognising that $\partial_s S(s, \theta) = \hat{t}(s) + \epsilon \partial_s[\rho(s)\hat{e}_\rho(s, \theta)]$, $\partial_\theta S(s, \theta) = \epsilon \rho(s)\partial_\theta \hat{e}_\rho(s, \theta)$ and $\hat{t} \times \partial_\theta \hat{e}_\rho = -\hat{e}_\rho$, and performing a Taylor expansion in ϵ. Physically, the single-layer kernel, K_t, describes the flow induced by a distribution of forces located on the surface of the body, while the double-layer kernel, K_s, can be interpreted as the flow created by a distribution of force dipoles and irrotational sources (see Kim & Karrila 2005).

In the slender limit, the kernels in (3.1)–(3.2) have two regions of behaviour: (i) an outer region, where $s - s' = O(1)$, and (ii) an inner region, where $s - s' = O(\epsilon)$. We therefore need to expand both kernels in these limits and match their values to determine the leading-order results. Throughout this expansion, higher-order contributions can also be determined by extending the Taylor series expansions further but have been omitted here for simplicity.

3.1. *Outer region*

In the outer region, $R_0(s, s')$ is assumed to be of order 1 and so $R \approx R_0$. Using the superscript (o) to indicate the outer-region expansion, the leading-order contributions to kernels in this region are

$$K_t^{(o)} = \rho(s') \frac{I + \hat{R}_0 \hat{R}_0}{|R_0|} \cdot f(s', \theta') + O(\epsilon), \tag{3.5}$$

$$K_s^{(o)} = 6\epsilon \rho(s') U(s', \theta') \cdot \frac{\hat{R}_0 \hat{R}_0 \hat{R}_0}{|R_0|^2} \cdot \hat{e}_\rho(s', \theta') + O(\epsilon^2), \tag{3.6}$$

where we have recognised that $\hat{n}_S(s', \theta') = -\hat{e}_\rho(s', \theta') + O(\epsilon)$ for slender bodies. Physically, this region captures the influence of surface points far from the point of interest, (s, θ).

3.2. *Inner region*

In the inner region, s' is assumed to be within $O(\epsilon)$ of s. Therefore, any dependence on s' can be Taylor expanded around s, leading to

$$\boldsymbol{R}_0 = -\epsilon \chi \hat{\boldsymbol{t}} + O(\epsilon^2), \tag{3.7}$$

$$\boldsymbol{f}(s', \theta') = \boldsymbol{f}(s, \theta') + O(\epsilon), \tag{3.8}$$

$$\rho(s') = \rho(s) + O(\epsilon), \tag{3.9}$$

$$\hat{\boldsymbol{e}}_\rho(s', \theta') = \hat{\boldsymbol{e}}_\rho(s, \theta') + O(\epsilon), \tag{3.10}$$

$$\boldsymbol{U}(s', \theta') = \boldsymbol{U}(s, \theta') + O(\epsilon), \tag{3.11}$$

where $\epsilon \chi = (s' - s)$. Using the superscript (i) to indicate inner-region expansions, the leading-order kernels in the inner region are therefore given by

$$\epsilon \boldsymbol{K}_t^{(i)} = \rho(s) \frac{\boldsymbol{I} + \hat{\boldsymbol{R}}^{(i)} \hat{\boldsymbol{R}}^{(i)}}{|\boldsymbol{R}^{(i)}|} \cdot \boldsymbol{f}(s, \theta') + O(\epsilon), \tag{3.12}$$

$$\epsilon \boldsymbol{K}_s^{(i)} = 6\rho(s) \boldsymbol{U}(s, \theta') \cdot \frac{\hat{\boldsymbol{R}}^{(i)} \hat{\boldsymbol{R}}^{(i)} \hat{\boldsymbol{R}}^{(i)}}{|\boldsymbol{R}^{(i)}|^2} \cdot \hat{\boldsymbol{e}}_\rho(s, \theta') + O(\epsilon), \tag{3.13}$$

where

$$\boldsymbol{R}^{(i)} = -\chi \hat{\boldsymbol{t}} + \rho(s)[\hat{\boldsymbol{e}}_\rho(s, \theta) - \hat{\boldsymbol{e}}_\rho(s, \theta')] = -\chi \hat{\boldsymbol{t}} + \rho(s) \Delta \hat{\boldsymbol{e}}_\rho(s, \theta, \theta'). \tag{3.14}$$

Physically, in this region, the slender body behaves locally like a cylinder, as reflected in the form of $\boldsymbol{R}^{(i)}$. As such, the expansion assumes that the curvature, $\kappa(s)$, is much less then $1/\epsilon$, a constraint identical to that assumed by Johnson (1979) and Götz (2000). Similar restrictions on the torsion do not occur at this order because of the definition of $\hat{\boldsymbol{e}}_\rho$.

The inner expansion also assumes that the change in the cross-section, $\partial_s \rho(s)$, is much less than $1/\epsilon$. This condition, however, is likely to be violated near the ends of the body. For example, bodies with ellipsoidal cross-sections, $\rho(s) = \sqrt{1 - s^2}$, have diverging $\partial_s \rho(s)$ at their ends. The significance of these end regions to the final integral can estimated using scaling arguments. We consider an end region of typical size $\sim \sigma$ in which $\epsilon \partial_s \rho(s) \sim O(1/\epsilon^{n-1})$ for $n \geqslant 1$. As the leading-order inner region is of $O(1/\epsilon)$, the contribution to the BI from this region scales as $\sigma \times (1/\epsilon^{n-1}) \times (1/\epsilon) \sim \sigma/\epsilon^n$. Hence, provided that $\sigma/\epsilon^n \lesssim O(\epsilon)$, end effects are small. For an ellipsoidal cross-section, $\partial_s \rho(s)$ becomes of $O(1/\epsilon^n)$ at $\sigma \sim \epsilon^{2n}$ away from the ends, thereby introducing a correction of $O(\epsilon^n)$. If, however, $\sigma/\epsilon^n \gtrsim O(1)$, a new region in which $\rho(s')$ cannot be expanded around $\rho(s)$ is needed to capture the influence of the ends.

3.3. *Common part*

Some of the behaviour in the expanded kernels is common to both the outer and inner regions. In order to identify this common behaviour, the relation $\epsilon \chi = s' - s$ is first used to rewrite either the inner-region expansion in terms of the outer-region variable, s', or the outer-region expansion in terms of inner-region variable, χ. The common part is then found by expanding the resultant kernel in ϵ. This method, known as the Van Dyke matching method (Hinch 1991), should produce the same result when

expanding the outer expansion in the inner variable or *vice versa*. For our problem, the common parts of the BI kernels are

$$\boldsymbol{K}_t^{(i)\in(o)} = \rho(s)\frac{\boldsymbol{I}+\hat{\tilde{\boldsymbol{t}}}\hat{\tilde{\boldsymbol{t}}}}{|s'-s|} \cdot \boldsymbol{f}(s,\theta') + O(\epsilon), \tag{3.15}$$

$$\boldsymbol{K}_s^{(i)\in(o)} = 6\epsilon\rho(s')\boldsymbol{U}(s,\theta') \cdot \frac{\hat{\tilde{\boldsymbol{t}}}\hat{\tilde{\boldsymbol{t}}}\hat{\tilde{\boldsymbol{t}}}}{|s'-s|^2} \cdot \hat{\boldsymbol{e}}_\rho(s,\theta') + O(\epsilon^2), \tag{3.16}$$

where the superscript $(i)\in(o)$ means that we expanded the inner-region kernels using the outer-region variable (the expansion of the outer-region kernel produces the same results).

3.4. *Total*

The outer and inner expansions and their common parts can be combined to create a composite representation of each of the BI kernels by adding the outer and inner expansions and then subtracting the common behaviour (Hinch 1991), thus allowing the composite representation to describe both the leading-order inner and outer behaviours in a single function. The composite representations of the kernels therefore allow the full BI equations to be approximated by

$$4\pi\boldsymbol{U}(s,\theta) \approx \int_{-1}^{1}\int_{-\pi}^{\pi} (\boldsymbol{K}_t^{(o)} + \boldsymbol{K}_t^{(i)} - \boldsymbol{K}_t^{(i)\in(o)} + \boldsymbol{K}_s^{(o)} + \boldsymbol{K}_s^{(i)} - \boldsymbol{K}_s^{(i)\in(o)}) \, \mathrm{d}\theta' \, \mathrm{d}s'. \tag{3.17}$$

In this leading-order representation, many of the s' integrals take the form

$$\int_{-1}^{1} \frac{\chi^i}{\epsilon\sqrt{\chi^2+\gamma^2}^j} \, \mathrm{d}s', \tag{3.18}$$

where $\epsilon\chi = s' - s$, γ is a constant with respect to s' (but can depend on s, θ and θ'), and i and j are positive integers. Integrals of this form can be evaluated exactly with the substitution $\chi = \gamma\sinh(\phi)$ and then expanded in ϵ to find the leading-order contribution (Koens & Lauga 2017). A list of the expansions relevant to this derivation is found in table 1. Significantly, the leading-order component of the asymptotic expansions of (3.18) is also the principal value of these integrals. Hence, the slender-body expansion of the BI representation leads to

$$
\begin{aligned}
4\pi\boldsymbol{U}(s,\theta) = \int_{-1}^{1} &\left(\frac{\boldsymbol{I}+\hat{\boldsymbol{R}}_0\hat{\boldsymbol{R}}_0}{|\boldsymbol{R}_0|} \cdot \langle\rho(s')\boldsymbol{f}(s')\rangle - \frac{\boldsymbol{I}+\hat{\tilde{\boldsymbol{t}}}\hat{\tilde{\boldsymbol{t}}}}{|s'-s|} \cdot \langle\rho(s)\boldsymbol{f}(s)\rangle \right) \mathrm{d}s' \\
&+ \int_{-\pi}^{\pi} \left[L(\boldsymbol{I}+\hat{\tilde{\boldsymbol{t}}}\hat{\tilde{\boldsymbol{t}}}) - 2\hat{\tilde{\boldsymbol{t}}}\hat{\tilde{\boldsymbol{t}}} + \frac{\Delta\hat{\boldsymbol{e}}_\rho\Delta\hat{\boldsymbol{e}}_\rho}{1-\cos(\theta'-\theta)} \right] \cdot \rho(s)\boldsymbol{f}(s,\theta') \, \mathrm{d}\theta' \\
&- 2\int_{-\pi}^{\pi} \left[\hat{\tilde{\boldsymbol{t}}}\hat{\tilde{\boldsymbol{t}}} + \frac{\Delta\hat{\boldsymbol{e}}_\rho\Delta\hat{\boldsymbol{e}}_\rho}{1-\cos(\theta'-\theta)} \right] \cdot \boldsymbol{U}(s,\theta') \, \mathrm{d}\theta' + O(\epsilon), \tag{3.19}
\end{aligned}
$$

where $L = \ln(2(1-s^2)/(\epsilon^2\rho^2(s)[1-\cos(\theta'-\theta)]))$, $\langle\boldsymbol{f}(s')\rangle = \int_{-\pi}^{\pi} \mathrm{d}\theta'\boldsymbol{f}(s',\theta')$ and the modulus sign has been dropped from the $1-\cos(\theta'-\theta)$ terms as they are always positive. In (3.19), the integrals of $\boldsymbol{K}_s^{(o)} - \boldsymbol{K}_s^{(i)\in(o)}$ have been omitted as they are order ϵ smaller than the other terms.

	$i = 0$	$i = 1$	$i = 2$
$j = 1$	$\log\left(\dfrac{4(1-s^2)}{\epsilon^2\gamma^2}\right)$	—	—
$j = 3$	$\dfrac{2}{\gamma^2}$	$\dfrac{2s\epsilon}{s^2-1}$	$\left[\log\left(\dfrac{4(1-s^2)}{\epsilon^2\gamma^2}\right) - 2\right]$
$j = 5$	$\dfrac{4}{3\gamma^4}$	0	$\dfrac{2}{3\gamma^2}$

TABLE 1. Asymptotic values of the integrals in (3.18) for different i and j up to $O(\epsilon^2)$.

It should be noted that the logarithmic term, L, diverges at the ends of the body, $|s| \to 1$, unless $\rho^2(s) \sim (1 - s^2)$. This suggests that ellipsoidal ends are the natural choice for the ends of the bodies in this expansion, and, indeed, for such shapes, a Taylor expansion of $\rho^2(s)$ near $|s| = 1$ leads to $\rho^2(s) \to 0$ and $\partial_s\rho^2(s) \to \partial_{ss}\rho^2(s)$. For non-ellipsoidal ends, the equations can still be used as the logarithmic singularity is integrable; however, to accurately capture the influence of the ends, an improved treatment may be required.

4. The SBT equations

The slender BI equation, equation (3.19), can be further simplified by expanding the surface velocity and traction in a Fourier series. Specifically, use of the general Fourier expansions

$$2\pi\boldsymbol{U}(s, \theta) = \boldsymbol{U}_0(s) + \sum_{n=1}^{\infty} \boldsymbol{U}_{c,n}(s)\cos[n(\theta - \theta_i)] + \boldsymbol{U}_{s,n}(s)\sin[n(\theta - \theta_i)], \quad (4.1)$$

$$2\pi\rho(s)\boldsymbol{f}(s, \theta) = \boldsymbol{f}_0(s) + \sum_{n=1}^{\infty} \boldsymbol{f}_{c,n}(s)\cos[n(\theta - \theta_i)] + \boldsymbol{f}_{s,n}(s)\sin[n(\theta - \theta_i)], \quad (4.2)$$

combined with the integral identities (Gradshteyn *et al.* 2000)

$$\int_0^{2\pi} d\theta \ln[1 - \cos(\theta)] = -2\pi \log(2), \quad (4.3)$$

$$\int_0^{2\pi} d\theta \ln[1 - \cos(\theta)]\cos(n\theta) = -\frac{2\pi}{n} \quad (n > 0), \quad (4.4)$$

$$\int_0^{2\pi} d\theta \ln[1 - \cos(\theta)]\sin(n\theta) = 0 \quad (n \geqslant 0), \quad (4.5)$$

allows all of the integrals involving θ' to be evaluated. For these Fourier expansions, subscript 0 represents the zeroth mode, subscript c, n represents the nth cosine mode and subscript s, n represents the nth sine mode. The orthogonality of trigonometric functions then reduces the zeroth-order Fourier mode of (3.19) to

850 R1-8

The boundary integral formulation of Stokes flows includes slender-body theory

$$4\boldsymbol{U}_0(s) = \int_{-1}^{1} \mathrm{d}s' \left(\frac{\boldsymbol{I} + \hat{\boldsymbol{R}}_0\hat{\boldsymbol{R}}_0}{|\boldsymbol{R}_0|} \cdot \boldsymbol{f}_0(s') - \frac{\boldsymbol{I} + \hat{\tilde{\boldsymbol{t}}}\boldsymbol{t}}{|s' - s|} \cdot \boldsymbol{f}_0(s) \right)$$
$$+ [L_{SBT}(\boldsymbol{I} + \hat{\tilde{\boldsymbol{t}}}\boldsymbol{t}) + \boldsymbol{I} - 3\hat{\tilde{\boldsymbol{t}}}\boldsymbol{t}] \cdot \boldsymbol{f}_0(s) + O(\epsilon), \tag{4.6}$$

while the higher-order Fourier modes lead to

$$2n\boldsymbol{U}_{c,n}(s) = (\boldsymbol{I} + \hat{\tilde{\boldsymbol{t}}}\boldsymbol{t}) \cdot \boldsymbol{f}_{c,n}(s) + O(\epsilon) \quad (n > 0), \tag{4.7}$$
$$2n\boldsymbol{U}_{s,n}(s) = (\boldsymbol{I} + \hat{\tilde{\boldsymbol{t}}}\boldsymbol{t}) \cdot \boldsymbol{f}_{s,n}(s) + O(\epsilon) \quad (n > 0), \tag{4.8}$$

where $L_{SBT} = \ln[4(1 - s^2)/(\epsilon^2\rho^2(s))]$. The equation above provides a relationship between the movement of the centreline and the average force per unit length on the fluid from the body, while the second and third relate more complex surface deformations to the corresponding surface tractions. Similarly to other SBT treatments, these relationships are either linear or a one-dimensional Fredholm equation of the second kind. Solutions to a boundary value problem are therefore determined by expanding the known surface distribution in a Fourier series in θ, inserting the Fourier coefficients into (4.6)–(4.8) to determine the coefficients of the unknown distribution and then reconstructing that distribution from (4.1) and (4.2). Importantly, the equation for the mean force per unit length, equation (4.6), is identical to the KRJ-SBT equation, equation (1.7). Johnson (1979) originally derived this equation by expanding the flow from a line distribution of stokeslets and potential source dipoles, and so this singularity representation captures the same physics as the BI representation when both are expanded in the slender-body limit.

A similar equivalence may be found for the torque per unit length generated from the surface rotation. For a cylindrical body, the surface velocity, surface traction and torque per unit length, $\boldsymbol{l}(s)$, resulting from the local rotation $\Omega\hat{\boldsymbol{t}}$ are given by

$$\boldsymbol{U}(s, \theta) = \epsilon\rho(s)\Omega\hat{\boldsymbol{t}} \times \hat{\boldsymbol{e}}_\rho(s, \theta) = \epsilon\rho(s)\Omega\hat{\boldsymbol{e}}_\theta(s, \theta), \tag{4.9}$$
$$\rho(s)\boldsymbol{f}(s, \theta) = 2\epsilon\rho(s)\Omega\hat{\boldsymbol{e}}_\theta(s, \theta), \tag{4.10}$$
$$\boldsymbol{l}(s) = \int_{-\pi}^{\pi} \mathrm{d}\theta\rho(s)[\boldsymbol{S}(s, \theta) \times \boldsymbol{f}(s, \theta)] = 4\pi\epsilon^2\rho^2(s)\Omega\hat{\boldsymbol{t}}, \tag{4.11}$$

where $\hat{\boldsymbol{e}}_\theta(s, \theta) = -\sin[\theta - \theta_i(s)]\hat{\boldsymbol{n}} + \cos[\theta - \theta_i(s)]\hat{\boldsymbol{b}}$. The above torque is identical to that derived from a line of singularities (Koens & Lauga 2014), showing again that the singularity and BI representations capture the same physics in the slender-body limit.

5. Single-layer and double-layer slender-body equations

Under certain conditions, the single-layer and double-layer potentials are also separately solutions to the Stokes equations and may be used to form modified BI equations (Pozrikidis 1992). Specifically, the single-layer BI representation is written as

$$8\pi\mu\boldsymbol{U}(\boldsymbol{x}) = \iint_S \mathrm{d}S(\boldsymbol{x}_0)[\boldsymbol{G}(\boldsymbol{R}) \cdot \boldsymbol{f}^m(\boldsymbol{x}_0)], \tag{5.1}$$

and holds when there is no flux of fluid through the boundaries. The double-layer BI is

$$8\pi\boldsymbol{U}(\boldsymbol{x}) = 4\pi\boldsymbol{U}^m(\boldsymbol{x}) + \iint_S^{PV} \mathrm{d}S(\boldsymbol{x}_0)[\boldsymbol{U}^m(\boldsymbol{x}_0) \cdot \boldsymbol{T}(\boldsymbol{R}) \cdot \hat{\boldsymbol{n}}_s(\boldsymbol{x}_0)], \tag{5.2}$$

and is valid when there is no net force or torque on bodies within the boundaries. In these equations, f^m is termed the modified surface traction on the fluid and U^m is the modified surface velocity. In numerical computations, these equations are often easier to evaluate than the full BI equations. It is therefore relevant to consider what SBT equations would arise from these two representations.

The general slender BI equation, equation (3.19), contains the expanded forms of the single-layer and double-layer potentials. The single-layer representation can, therefore, be found by replacing the 4π on the left-hand side with 8π, the surface traction with the modified traction, $f \to f^m$, and the velocities on the right-hand side with zero, $U = 0$. The resultant single-layer SBT equation is given for the mean as

$$4U_0(s) = \int_{-1}^{1} \mathrm{d}s' \left(\frac{I + \hat{R}_0\hat{R}_0}{|R_0|} \cdot f_0^m(s') - \frac{I + \hat{t}\hat{t}}{|s' - s|} \cdot f_0^m(s) \right)$$
$$+ [L_{SBT}(I + \hat{t}\hat{t}) + I - 3\hat{t}\hat{t}] \cdot f_0^m(s) + O(\epsilon), \tag{5.3}$$

while for the other Fourier modes we now have

$$8U_{c,1}(s) = [2(I + \hat{t}\hat{t}) - \hat{n}\hat{n} + \hat{b}\hat{b}] \cdot f_{c,1}^m(s) - (\hat{n}\hat{b} + \hat{b}\hat{n}) \cdot f_{s,1}^m(s) + O(\epsilon), \tag{5.4}$$

$$8U_{s,1}(s) = [2(I + \hat{t}\hat{t}) + \hat{n}\hat{n} - \hat{b}\hat{b}] \cdot f_{s,1}^m(s) - (\hat{n}\hat{b} + \hat{b}\hat{n}) \cdot f_{c,1}^m(s) + O(\epsilon), \tag{5.5}$$

$$4nU_{c,n}(s) = (I + \hat{t}\hat{t}) \cdot f_{c,n}^m(s) + O(\epsilon) \quad (n > 1), \tag{5.6}$$

$$4nU_{s,n}(s) = (I + \hat{t}\hat{t}) \cdot f_{s,n}^m(s) + O(\epsilon) \quad (n > 1), \tag{5.7}$$

where we have written the modified traction and the surface velocity as Fourier series.

The equation for the mean force per unit length is structured exactly like KRJ-SBT; the torque per unit length from surface rotation can be shown to also be the same as (4.11). The difference between the single-layer and full BI representations occurs for the $n = 1$ Fourier terms. In the full BI representation, every force mode was uniquely related to a surface deformation. However, in the single-layer representation, the $n = 1$ equations do not fully determine $f_{c,1}^m$ and $f_{s,1}^m$ since these equations have no solution for $f_{c,1}^m \cdot \hat{n}$ and $f_{s,1}^m \cdot \hat{b}$ unless $U_{c,1} \cdot \hat{n} + U_{s,1} \cdot \hat{b} = 0$. This restriction implies that solutions exist only if $\int_{-\pi}^{\pi} \mathrm{d}\theta U \cdot \hat{e}_\rho = 0$, thereby preventing any local changes in the body volume. The inability of the single-layer SBT to uniquely determine the $n = 1$ modes reflects the inability of the single-layer BI to describe bodies with changing volume (Pozrikidis 1992).

Similarly, the double-layer SBT equations can be obtained from (3.19) by setting the traction to zero, $f = 0$, replacing the velocity on the right-hand side of the equation with the modified surface velocity $U \to U^m$, adding $4\pi U^m$ to the right-hand side and replacing the 4π with 8π on the left-hand side. The double-layer SBT equations then become

$$4U_0(s) = 0 + O(\epsilon), \tag{5.8}$$

$$4U_{c,1}(s) = [2I + \hat{n}\hat{n} - \hat{b}\hat{b}] \cdot U_{c,1}^m(s) + (\hat{n}\hat{b} + \hat{b}\hat{n}) \cdot U_{s,1}^m(s) + O(\epsilon), \tag{5.9}$$

$$4U_{s,1}(s) = [2I + \hat{b}\hat{b} - \hat{n}\hat{n}] \cdot U_{s,1}^m(s) + (\hat{n}\hat{b} + \hat{b}\hat{n}) \cdot U_{c,1}^m(s) + O(\epsilon), \tag{5.10}$$

$$4U_{c,n}(s) = 2U_{c,n}^m + O(\epsilon) \quad (n > 1), \tag{5.11}$$

$$4U_{s,n}(s) = 2U_{s,n}^m + O(\epsilon) \quad (n > 1), \tag{5.12}$$

where we have again expanded the functions in Fourier components. Similarly to the single-layer slender-body equations, the double-layer equations have solutions only if $U_0 = 0$ and $\int_{-\pi}^{\pi} \mathrm{d}\theta U \cdot \hat{e}_\theta = 0$, reflecting the inability of the double-layer BI to describe bodies with either net forces or torques.

6. Conclusion

The Green's function for the Stokes equations allows low-Reynolds-number flows to be represented mathematically using either BIs or distributions of singularities. Boundary integrals are an effective general procedure for many shapes but are difficult to implement computationally for slender bodies. In contrast, singularity representations require suitable guesses of the relevant singularities but are useful in order to construct theories for the hydrodynamics of long slender bodies (denoted SBTs).

In this paper, we derive an algebraically accurate SBT directly from the BI representation for Stokes flows. This derivation (i) requires no consideration about the type, strength or location of the singularities, (ii) is a direct result of the Stokes equations and (iii) provides an SBT that relates arbitrary surface velocities to arbitrary surface tractions. The equation for the mean force and torque per unit length has the same structure as the SBTs of Keller & Rubinow (1976) and Johnson (1979), demonstrating that a representation consisting of placing singularities over the centreline of a body and the BI representation describe the same physics when expanded in the slender-body limit.

Our derivation was first obtained from the most general BI representation before being adapted to both the single-layer and double-layer boundary representations. The equations for the mean force per unit length and mean torque per unit length are the same across the different representations. While the full BI representation is able to handle any surface velocity, it was found that the single-layer representation only has solutions if the body does not locally change volume, and the double-layer representation only has solutions if there is no local translation or surface rotation of the filament. Both of these conditions are the SBT equivalents of the restrictions on modified BIs. Importantly, as this theory handles arbitrary surface velocities and tractions, this formalism can be applied to non-rigid bodies and bodies near neighbours by including the relevant additional terms.

Acknowledgements

References

BARTA, E. & LIRON, N. 1988 Slender body interactions for low Reynolds numbers. Part I: body–wall interactions. *SIAM J. Appl. Maths* **48**, 992–1008.

BATCHELOR, G. K. 1970 Slender-body theory for particles of arbitrary cross-section in Stokes flow. *J. Fluid Mech.* **44**, 419–440.

CHWANG, A. T. & WU, T. Y. 1975 Hydromechanics of low-Reynolds-number flow. Part 2. Singularity method for Stokes flows. *J. Fluid Mech.* **67**, 787–815.

CLARKE, N. S. 1972 The force distribution on a slender twisted particle in a Stokes flow. *J. Fluid Mech.* **52**, 781–793.

COX, R. G. 1970 The motion of long slender bodies in a viscous fluid. Part 1. General theory. *J. Fluid Mech.* **44**, 791–810.

GÖTZ, T. 2000 Interactions of fibers and flow: asymptotics, theory and numerics. PhD thesis, University of Kaiserslautern, Kaiserslautern, Germany.

GRADSHTEYN, I. S., RYZHIK, I. M., JEFFREY, A. & ZWILLINGER, D. 2000 *Table of Integrals, Series, and Products*. Academic Press.

GUO, H., FAUCI, L., SHELLEY, M. & KANSO, E. 2018 Bistability in the synchronization of actuated microfilaments. *J. Fluid Mech.* **836**, 304–323.

HINCH, E. J. 1991 *Perturbation Methods*. Cambridge University Press.

JOHNSON, R. E. 1979 An improved slender-body theory for Stokes flow. *J. Fluid Mech.* **99**, 411–431.

KELLER, J. B. & RUBINOW, S. I. 1976 Slender-body theory for slow viscous flow. *J. Fluid Mech.* **75**, 705–714.

KIM, S. & KARRILA, S. J. 2005 *Microhydrodynamics: Principles and Selected Applications*. Courier Corporation.

KOENS, L. & LAUGA, E. 2014 The passive diffusion of Leptospira interrogans. *Phys. Biol.* **11**, 066008.

KOENS, L. & LAUGA, E. 2016 Slender-ribbon theory. *Phys. Fluids* **28**, 013101.

KOENS, L. & LAUGA, E. 2017 Analytical solutions to slender-ribbon theory. *Phys. Rev. Fluids* **2**, 084101.

LIGHTHILL, J. 1976 Flagellar hydrodynamics: the John von Neumann lecture, 1975. *SIAM Rev.* **18**, 161–230.

MYERSCOUGH, M. & SWAN, M. 1989 A model for swimming unipolar spirilla. *J. Theor. Biol.* **139**, 201–218.

POZRIKIDIS, C. 1992 *Boundary Integral and Singularity Methods for Linearized Viscous Flow*. Cambridge University Press.

SELLIER, A. 1999 Stokes flow past a slender particle. *Proc. R. Soc. Lond.* A **455**, 2975–3002.

SMITH, D. J., GAFFNEY, E. A., BLAKE, J. R. & KIRKMAN-BROWN, J. C. 2009 Human sperm accumulation near surfaces: a simulation study. *J. Fluid Mech.* **621**, 289–320.

TORNBERG, A. & GUSTAVSSON, K. 2006 A numerical method for simulations of rigid fiber suspensions. *J. Comput. Phys.* **215**, 172–196.

TORNBERG, A. & SHELLEY, M. J. 2004 Simulating the dynamics and interactions of flexible fibers in Stokes flows. *J. Comput. Phys.* **196**, 8–40.